*Quantum Electronics* **44** (7) 700–702 (2014)

***FIBRE-OPTIC AND NONLINEAR OPTICAL INSTRUMENTS***

PACS numbers: 42.55.Wd; 42.60.Da; 42.81.Wg
DOI: 10.1070/QE2014v044n07ABEH015573

# Superfluorescent 1.34 μm bismuth-doped fibre source

K.E. Riumkin, M.A. Mel'kumov, A.V. Shubin, S.V. Firstov, I.A. Bufetov,
V.F. Khopin, A.N. Gur'yanov, E.M. Dianov

***Abstract.*** **We have demonstrated the first superfluorescent fibre source emitting in the 1.34 μm range. In a double-pass configuration with an amplifier, its output power is 48 mW under pumping at $\lambda = 1240$ nm. Its emission spectrum has a nearly Gaussian shape, with a full width at half maximum of 26 nm at the highest pump power.**

***Keywords:*** *bismuth, optical fibre, superfluorescent fibre source.*

Superfluorescent fibre sources (SFS's) find wide application in many areas of science and technology: in fibre-optic gyroscopes, ophthalmology, optical time-domain reflectometry, optical telecommunications and devices that need a signal with low temporal coherence and high spatial coherence. Requirements for SFS's stem from the application they are intended for. In particular, it is necessary for the operation of precision fibre-optic gyroscopes that the output bandwidth of the SFS's be in excess of 15 nm and that their output power be at least 10 mW, in combination with sufficiently high optical efficiency. Moreover, the signal should have a stable mean wavelength, insensitive to variations in temperature and other external factors.

Most of these requirements are met by superfluorescent rare-earth-doped fibre sources, the most widespread of which are erbium-, ytterbium-, thulium- and neodymium-doped [1].

The development of 1.3-μm broadband fibre sources is hindered by the fact that no rare-earth elements have high gain transitions in this range. Only one SFS, based on praseodymium-doped fluorozirconate (ZBLAN) fibre, has so far been demonstrated in this spectral region [2]. Amplified spontaneous emission (ASE) on the $^1G_4 \rightarrow {}^3H_5$ transition was observed at a wavelength of 1.306 μm under direct excitation from the $^1G_4$ metastable level by the 1.017-μm Ti : sapphire laser line. In a single-pass configuration, the output power of the SFS was just 0.166 mW at a pump power of 540 mW. The conversion efficiency was so low because of the low luminescence quantum yield (about 3%).

One possible solution to the problem is to use semiconductor superluminescent laser diodes, which are available for almost any wavelength in the range 0.4 to 2.0 μm. Unfortunately, they have a number of drawbacks: limited output power, low temperature stability of their mean wavelength, marked modulation of their emission spectrum, small energy conversion coefficient at long wavelengths and residual polarisation of their output.

Bismuth-doped fibres offer rather high efficiency and appear to be a promising active medium for creating SFS's in new optical ranges. Another advantage is that different glass hosts enable amplification in different wavelength ranges: 1.14–1.22 (aluminosilicate host), 1.25–1.35 (phosphosilicate host), 1.32–1.55 (germanosilicate host) and 1.63–1.77 μm (silicogermanate host) [3–6].

The first superfluorescent bismuth-doped germanosilicate fibre source was reported in Ref. [7]. The SFS had a mean wavelength of 1.44 μm and a bandwidth of 25 nm at an output power of 82 mW, and its optical efficiency was 31%.

Here, we demonstrate a superfluorescent phosphosilicate fibre source with a mean output wavelength of 1336 nm. A fibre preform was produced by MCVD and had a core–cladding refractive index difference $\Delta n = 5.5\times10^{-3}$ and a Bi concentration in the core below 0.1 wt %. The cutoff wavelength of the fibre was about 0.9 μm. Its absorption and gain spectra are presented in Fig. 1. At a pump wavelength of 1240 nm, the small-signal optical absorption in the fibre is 0.6 dB m$^{-1}$. At signal powers above 50 mW, the absorption drops to 0.09 dB m$^{-1}$. Under 1240-nm pumping, the highest gain is 0.2 dB m$^{-1}$ at 1320 nm.

The SFS consists of two stages: signal source and amplifier. The first stage has a double-pass, backward pumping

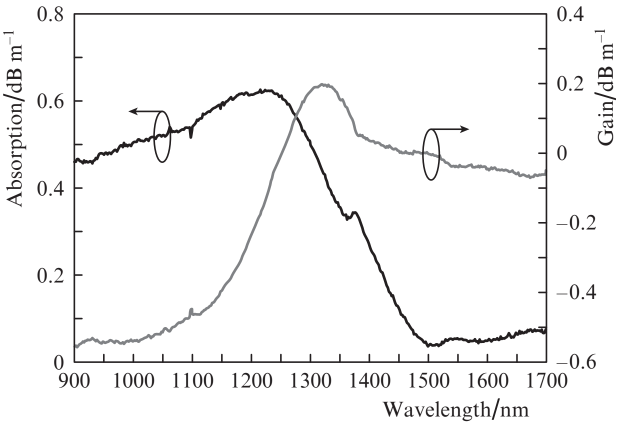

**Figure 1.** Absorption and gain spectra of the fibre.

**K.E. Riumkin, M.A. Mel'kumov, A.V. Shubin, S.V. Firstov, I.A. Bufetov, E.M. Dianov** Fiber Optics Research Center, Russian Academy of Sciences, ul. Vavilova 38, 119333 Moscow, Russia;
e-mail: riumkin@fo.gpi.ru;
**V.F. Khopin, A.N. Gur'yanov** G.G. Devyatykh Institute of Chemistry of High-Purity Substances, Russian Academy of Sciences, ul. Tropinina 49, 603950 Nizhnii Novgorod, Russia

Received 30 May 2014; revision received 19 June 2014
*Kvantovaya Elektronika* **44** (7) 700–702 (2014)
Translated by O.M. Tsarev

configuration (Fig. 2, top left), which was chosen by virtue of its higher efficiency and lower ASE threshold in comparison with single-pass SFS's. As a pump source, we used a 1240-nm laser diode with 300 mW of output power. The pump radiation was launched into the active fibre through a 1240/1340 nm WDM coupler. The active-fibre length (150 m) was chosen such as to maximise the SFS efficiency at the specified pump power. The fibre end had a fibre loop mirror (broadband 50/50 fused fibre coupler with connected output ports). To reduce the effect of the return signal, a fibre-optic isolator was placed at the output of the first stage.

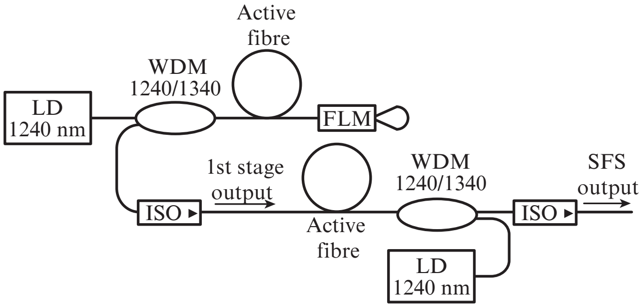

**Figure 2.** SFS configuration: (LD) laser diode, (WDM) wavelength division multiplexing coupler, (ISO) optical isolator, (FLM) fibre loop mirror.

Output spectra were measured with an Agilent 86140B spectrum analyser, and the output power was measured with an EXFO FPM-600 power meter.

Figure 3 shows output spectra of the SFS at various pump powers. With increasing pump power, the output spectrum becomes narrower and the mean wavelength increases (Fig. 4). At low pump powers, the gain in the fibre is low and, because the backward pumping configuration is used, the output of the first stage is contributed primarily by unamplified luminescence of a small section of the active fibre, which absorbs most of the pump power. The peak of this luminescence lies at 1.32 μm and is slightly shifted with respect to the peak emission wavelength of bismuth in a phosphosilicate host (1.3 μm) by virtue of reabsorption. With increasing pump power, the length of the fibre section with population inversion increases, an ASE occurs, and the output spectrum shifts to longer wavelengths, to the region where active bismuth centres have a maximum gain. The mean wavelength stabilises at a pump power of 260 mW and remains essentially unchanged at higher pump powers. The ASE threshold is about 150 mW. Figure 5 shows the output power of the SFS as a function of pump power.

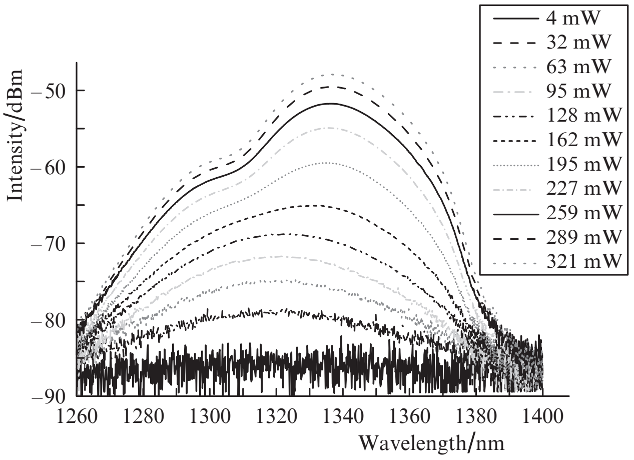

**Figure 3.** Output spectra of the first stage of the SFS at various pump powers.

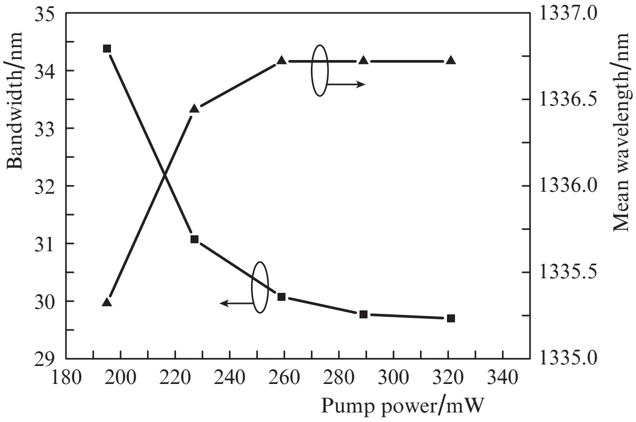

**Figure 4.** Bandwidth $\Delta\lambda_{\mathrm{FWHM}}$ and mean wavelength as functions of pump power for the output spectrum of the first stage of the SFS.

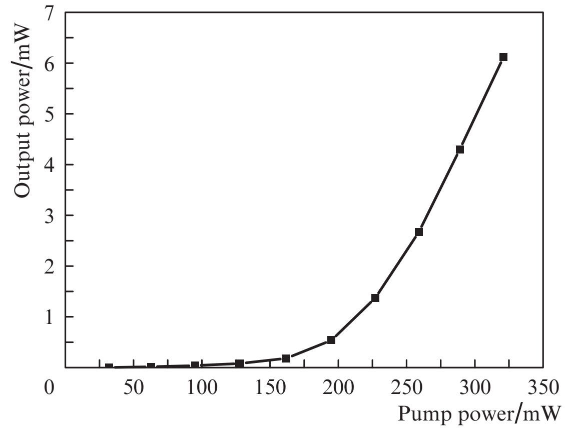

**Figure 5.** Output power of the first stage of the SFS as a function of pump power.

To reach a higher output power of the SFS, we used an additional amplification stage: a 120-m length of bismuth-doped active fibre pumped by a 1240-nm laser diode. To prevent lasing and reduce the effect of the return signal on the output parameters of the SFS, a fibre-optic isolator was placed at the output of this stage.

The output spectra of the SFS at various pump powers in the second amplification stage and the spectrum of the input signal are presented in Fig. 6.

The output power of the SFS increases linearly with the pump power in the second stage, reaching 48 mW at a pump power of 300 mW (Fig. 7). The mean wavelength is 1336 nm, and the bandwidth is $\Delta\lambda_{\mathrm{FWHM}} \approx 26$ nm (Fig. 8). At low pump powers in the second stage, there is no population inversion in most of the fibre, and some of the emission from the first stage is absorbed by active centres. As a result, only the longer

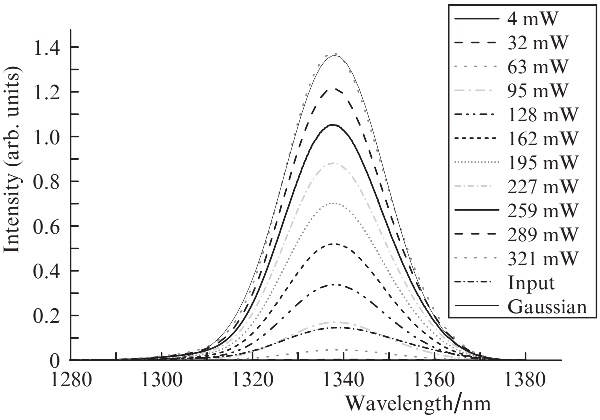

**Figure 6.** Output spectra of the SFS at various pump powers (on this intensity scale, the output spectra at pump powers of 4 and 32 mW essentially coincide with the abscissa).

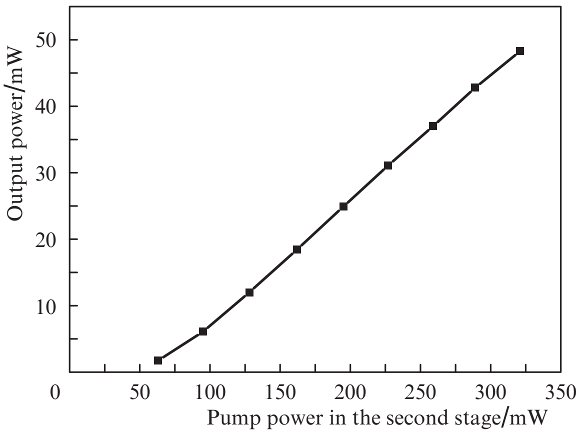

**Figure 7.** Output power of the SFS as a function of pump power.

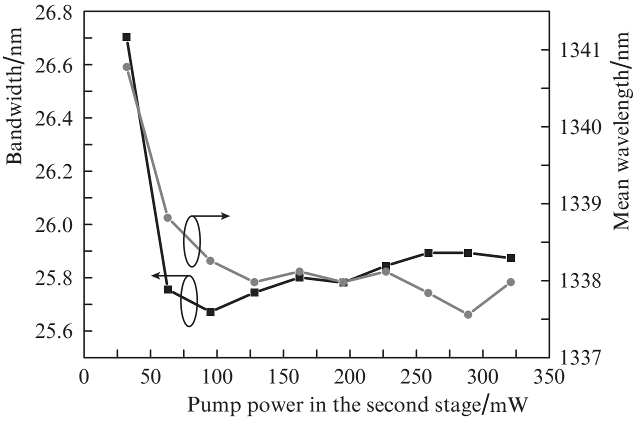

**Figure 8.** Bandwidth $\Delta\lambda_{\mathrm{FWHM}}$ and mean wavelength as functions of pump power for the output spectrum of the SFS.

wavelength part of the output spectrum persists, i.e. the emission peak is shifted to longer wavelengths with respect to the input signal. Note that the emission of active bismuth centres in the second stage is markedly weaker than the signal from the first stage. With increasing pump power, population inversion occurs throughout the length of the fibre and the output spectrum shifts to shorter wavelengths, to the peak gain region of the active bismuth centres.

Thus, we have demonstrated a superfluorescent bismuth-doped fibre source with an output mean wavelength of 1336 nm and a bandwidth of 26 nm FWHM at the highest pump power. Its output power is 48 mW at a net pump power of 600 mW, and its emission spectrum has a nearly Gaussian shape (a fit of its spectrum by a Gaussian at a pump power of 320 mW is shown in Fig. 6). We have demonstrated the first SFS operating in the region of the second transmission window (1.3 μm) of silica fibres and comparable in efficiency to widely used superfluorescent rare-earth-doped fibre sources. It is worth noting that this is only one possible implementation of superfluorescent bismuth-doped phosphosilicate fibre sources. The configuration can be optimised to meet particular requirements for the output signal.

***Acknowledgements.*** This work was supported by the Presidium of the Russian Academy of Sciences (Programme No. 24) and the Russian Foundation for Basic Research (Grant No. 13-02-01320A).

## References

1. Digonnet M.J.F. *Rare-Earth-Doped Fiber Lasers and Amplifiers* (New York: Marcel Dekker, Inc., 2001).
2. Ohishi Y., Kanamori T., Takahashi S. *Jpn. J. Appl. Phys.*, **30**, L1282 (1991).
3. Dianov E.M., Mel'kumov M.A., Shubin A.V., Firstov S.V., Khopin V.F., Gur'yanov A.N., Bufetov I.A. *Kvantovaya Elektron.*, **39**, 1099 (2009) [*Quantum Electron.*, **39**, 1099 (2009)].
4. Bufetov I.A., Melkumov M.A., Khopin V.F., Firstov S.V., Shubin A.V., Medvedkov O.I., Guryanov A.N., Dianov E.M. *Proc. SPIE Int. Soc. Opt. Eng.*, **7580**, 758014 (2010).
5. Bufetov I.A., Dianov E.M. *Laser Phys. Lett.*, **6**, 487 (2009).
6. Dianov E.M., Firstov S.V., Alyshev S.V., Riumkin K.E., Shubin A.V., Khopin V.F., Gur'yanov A.N., Medvedkov O.I., Mel'kumov M.A. *Kvantovaya Elektron.*, **44** (6), 503 (2014) [*Quantum Electron.*, **44** (6), 503 (2014)].
7. Riumkin K.E., Melkumov M.A., Bufetov I.A., Shubin A.V., Firstov S.V., Khopin V.F., Guryanov A.N., Dianov E.M. *Opt. Lett.*, **37**, 4817 (2012).